Structure, Vol. 9, 869–880, September, 2001, ©2001 Elsevier Science Ltd. All rights reserved. PII S0969-2126(01)00644-X

Crystal Structure of β-Arrestin at 1.9 Å: Possible Mechanism of Receptor Binding and Membrane Translocation

May Han,[1,4,5,6] Vsevolod V. Gurevich,[2] Sergey A. Vishnivetskiy,[2] Paul B. Sigler,[1,3] and Carsten Schubert[1,3,4,5,7]

[1] Department of Molecular Biophysics and Biochemistry
Yale University
New Haven, Connecticut 06520

[2] Ralph and Muriel Roberts Laboratory for Vision Science
Sun Health Research Institute
Sun City, Arizona 85372

[3] Howard Hughes Medical Institute

Summary

Background: Arrestins are responsible for the desensitization of many sequence-divergent G protein-coupled receptors. They compete with G proteins for binding to activated phosphorylated receptors, initiate receptor internalization, and activate additional signaling pathways.

Results: In order to understand the structural basis for receptor binding and arrestin's function as an adaptor molecule, we determined the X-ray crystal structure of two truncated forms of bovine β-arrestin in its cytosolic inactive state to 1.9 Å. Mutational analysis and chimera studies identify the regions in β-arrestin responsible for receptor binding specificity. β-arrestin demonstrates high structural homology with the previously solved visual arrestin. All key structural elements responsible for arrestin's mechanism of activation are conserved.

Conclusions: Based on structural analysis and mutagenesis data, we propose a previously unappreciated part in β-arrestin's mode of action by which a cationic amphipathic helix may function as a reversible membrane anchor. This novel activation mechanism would facilitate the formation of a high-affinity complex between β-arrestin and an activated receptor regardless of its specific subtype. Like the interaction between β-arrestin's polar core and the phosphorylated receptor, such a general activation mechanism would contribute to β-arrestin's versatility as a regulator of many receptors.

Introduction

Signal transduction pathways involving G protein-coupled receptors (GPCRs) control many vital processes of life, such as perception, hormone and neurotransmitter action, angiogenesis, and behavior. The human genome encodes ~1000 GPCRs and numerous G protein subunits. GPCR-mediated signaling is the most common way for cells to receive chemical signals from the extracellular environment. Arrestins play a central role in controlling the amplitude and duration of the GPCR signaling. Arrestins bind exclusively to activated and phosphorylated GPCRs. They terminate the primary signal transduction event by preventing further interaction of G proteins with the receptor. The arrestin family consists of visual arrestin (v-arrestin), cone arrestin, β-arrestin (synonyms, β-arrestin 1 and arrestin-2), and β-arrestin2 (synonym, arrestin3). V- and cone arrestins are exclusively expressed in rod and cone photoreceptors, respectively. They are highly specialized to bind specifically to rhodopsin, or cone cell pigments. The structure of v-arrestin was reported [1, 2]. The two closely related β-arrestins are ubiquitously expressed and are responsible for the termination of the primary signaling event for most, if not all, class I GPCRs. They also interact with clathrin and the AP2 adaptor protein to trigger receptor sequestration into clathrin-coated pits [3–5]. β-arrestin also interacts with the N-ethylmaleimide-sensitive fusion protein, linking receptor sequestration and vesicular transport [6]. Furthermore, it was shown that β-arrestin binds to the SH3 and catalytic domains of c-Src kinase in a receptor activation-dependent manner [7, 8]. This interaction provides a crucial link between the GPCR pathway and the mitogen-activated protein kinase (MAPK) pathways. In addition, β-arrestin is involved in regulation of mitogenic signaling and endocytosis of the IGF-1 receptor, a non-GPCR [9].

β-arrestin knockout (−/−) mice display altered cardiac responsiveness to β-adrenergic receptor stimulation [10]. β-arrestin2 knockout (−/−) mice demonstrate enhanced morphine analgesia [11]. Neither knockout displays an apparent abnormality, implying that there is functional redundancy between these two proteins. This hypothesis is supported by the fact that the two genes show extensive tissue expression overlap [12] and functional redundancy in that they bind many receptors with comparable affinity [13]. However, a double knockout of both β-arrestins is embryonic lethal [14]. Similarly, knockouts (−/−) of *kurtz*, a β-arrestin analog in *Drosophila*, display a broad lethal phase during embryogenesis [15].

Despite common molecular architecture and a few highly conserved residues scattered within the transmembrane segments, the sequence homology among all GPCRs is very low. The structural basis of β-arrestin's ability to interact with hundreds of different receptors is unknown.

Here we report the expression, purification, and crystallization of bovine β-arrestin in two truncated forms: β-arrestin 1–393 and 1–382, lacking the last 25 and 36 amino acids, respectively. The overall structure of β-arrestin is similar to that of visual arrestin [1]: an elon-

[4] Correspondence: mhan@mpi.com (M. H.), schubert@3dp.com (C. S.)
[5] These authors contributed equally to this work.
[6] Present address: Millennium Pharmaceuticals, Inc., 75 Sidney Street, Cambridge, Massachusetts 02139.
[7] Present address: 3-Dimensional-Pharmaceuticals Inc., 665 Stockton Drive, Exton, Pennsylvania 19341.

Key words: arrestin; X-ray crystallography; GPCR; signal transduction; membrane proteins

Table 1. Data Collection Statistics

Molecule	β-arrestin 1–393			β-arrestin 1–393	β-arrestin 1–382
Cell parameters	$P2_1$ a = 62.4 Å, b = 73.7 Å, c = 115.8 Å, α = γ = 90°, β = 98.7°			$P3_221$ a = b = 77.8 Å, c = 157.1 Å α = β = 90°, γ = 120°	$P2_1$ a = 62.4 Å, b = 73.3 Å, c = 115.3 Å, α = γ = 90°, β = 98°
Collection Strategy	SAD	High resolution[a]	Native	SAD	Native
Resolution (Å)	34–2.1	31–1.9	35–1.96	34–2.2	31–2.0
Wavelength (Å)	0.979	1.1	1.105	0.9785	1.1
Observations/Unique	387,810/58,960	238,590/68,946	158,905/49,309	267,488/27,920	226,069/68,102
R_{sym} (%)[b,c]	8.0 (46.2)	5.0 (46.6)	4.7 (46.8)	4.6 (45.6)	5.9 (48.2)
R_{meas} (%)[b,d]	8.7 (50.9)	5.9 (58.8)	5.6 (58.3)	4.8 (52.9)	7.0 (59.0)
Redundancy[b]	6.6 (5.2)	3.5 (2.2)	3.2 (1.5)	9.6 (3.8)	3.3 (2.5)
Completeness (%)[b]	96.9 (88.2)	84.5 (35.4)	65.8 (3.6)	94.7 (79.2)	95.1 (91)
I/σ[b,e]	5.6 (1.8)	7.3 (1.3)	7.5 (1.1)	10.4 (1.5)	5.8 (1.4)
HA-Refinement		SIRAS		SAD	
Resolution (Å)	34–1.9			34–2.2	
R_{iso} (%)[f]	8.7		12.9	—	
f′/f″	−20.5/9.7			−4.05/3.05	
Phasing power$_{cen/iso}$[g]	0.39	—	0.22	—	
Phasing power$_{acen/iso}$[g]	0.56	—	0.2	—	
Phasing power$_{acen/ano}$[g]	1.1	—	—	1.3	
Figures of merit[h]	0.14 (centrics) 0.2 (acentrics)			0.07 (centrics) 0.25 (acentrics)	

[a] Reference data set in heavy-atom refinement.

[b] Values for the highest resolution shell are given in parentheses.

[c] $R_{sym} = \frac{\sum_h \sum_i^{n_h} |\hat{I}h - Ih,i|}{\sum_h \sum_i^{n_h} Ih,i}$ with $\hat{I}h = \frac{1}{n_h} \sum_i^{n_h} Ih,i$, where I is the integrated intensity of a given reflection, and n is the n^{th} symmetry or Friedel equivalent.

[d] $R_{meas} = \frac{\sum_h \sqrt{\frac{n_h}{n_h - 1}} \sum_i^{n_h} |\hat{I}h - Ih,i|}{\sum_h \sum_i^{n_h} Ih,i}$, where n_h is the redundancy.

[e] Based on unmerged data.

[f] $R_{iso} = \Sigma|F_{PH} - F_P|/\Sigma F_P$, where F_P and F_{PH} are the native and derivative structure factor amplitudes.

[g] Phasing power = <rms heavy-atom structure factor>/<rms lack of closure>

[h] Figure of merit = weighted mean of the cosine of the deviation from α_{best}

gated molecule with a central polar core flanked by the N and C domains and a C tail connecting the two domains. Structural variations were mostly found in surface loops. The crystal structures suggest two possible mechanisms promoting receptor-arrestin interaction that are independent of the specific GPCR subtype. One mechanism is linked to the polar core, where critical salt bridges keep arrestin in its basal state [1]. An activated and phosphorylated GPCR would interact with arrestin, thereby disrupting the polar core and triggering the conformational changes required for high-affinity receptor binding. Based on structural and mutagenesis data, we propose a second general mechanism whereby receptor binding is triggered and/or enhanced by the membrane translocation of arrestin's amphipathic α helix I.

Results and Discussion

Structure of β-Arrestin

The crystallographic statistics are summarized in Table 1. Large crystals of trigonal morphology were obtained from wild-type bovine β-arrestin but did not diffract beyond 9 Å. β-arrestin 1–393, lacking the last 25 amino acids, is biochemically indistinguishable from the wild-type arrestin [16]. This truncated form yielded crystals of similar trigonal morphology belonging to space group $P3_221$, with one molecule per asymmetric unit. The limit of diffraction was 2.2 Å. β-arrestin 1–393 also yielded crystals of space group $P2_1$, with two molecules per asymmetric unit that diffracted to 1.9 Å. The structures of both crystal forms were solved by molecular replacement using v-arrestin as the search model and were refined against external phases obtained from single wavelength anomalous dispersion (SAD) experiments to minimize model bias (Figure 1; Table 2). We also crystallized β-arrestin 1–382, which was shown to exhibit phosphorylation-independent receptor binding due to the removal of the key regulatory residues [16]. β-arrestin 1–382 exists in solution as a mixture of dimers and monomers that can be separated by gel-filtration chromatography. Both dimeric and monomeric β-arrestin 1–382 yielded only monoclinic crystals with the same cell dimension as the $P2_1$ crystal form of β-arrestin 1–393 and diffracted to 2.4 Å and 1.9 Å, respectively. The structures were solved by molecular replacement and were found to be essentially identical to the search model, the $P2_1$ form of β-arrestin 1–393.

An overlay of β-arrestin structures (the $P3_221$ form and the α and β molecules of the dimer in the $P2_1$ form of β-arrestin 1–393 [Figure 2a, gold]) together with two

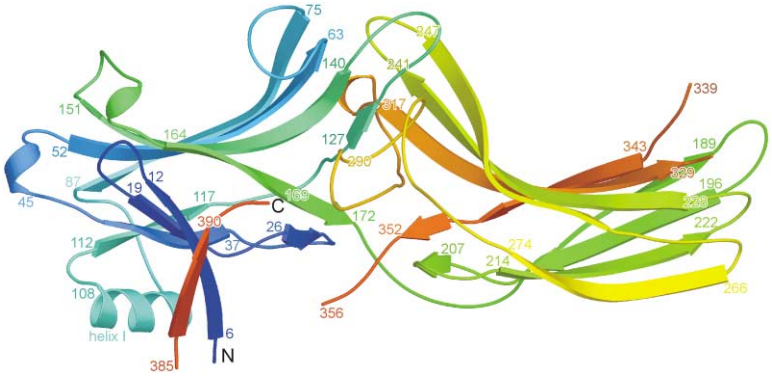

Figure 1. Ribbon Diagram of β-arrestin

The N and C termini are indicated by N and C, respectively. The color varies from blue to red as one goes from the N terminus to the C terminus. Figure generated with MOLSCRIPT/RASTER3D [69, 70].

structures of v-arrestin (Figure 2a, magenta) [1] demonstrates that the overall structure of β-arrestin is very similar to that of v-arrestin. The loop regions that vary between β-arrestin and v-arrestin also vary between different crystal forms of the same protein, reflecting the intrinsic flexibility of those regions rather than inherent structural differences between the two arrestins. As with v-arrestin [1], the crystal structure of β-arrestin represents its inactive basal state, where the polar core is intact. The unique sequence between residues 357–382 in β-arrestins, which contains the clathrin binding site, is disordered in all crystal forms. Interestingly, almost all of the residues (334–340) absent in a short splice variant of β-arrestin [12, 17] are also disordered.

The polar core, which has been shown to keep v-arrestin in its basal conformation [1], is structurally conserved in β-arrestin. The "lariat" loop (Figure 2b, blue, 282–309) is highly conserved among all arrestins and contains the primary counterion D290 for R169 in the polar core. It is a long stretch of amino acids apparently lacking any secondary structure, yet its tertiary structure is virtually identical in v-arrestin and β-arrestin . The charge reversal mutant D296R in v-arrestin (the equivalent of D290R in β-arrestin) demonstrates phosphorylation-independent receptor binding [1, 18]. The conserved structure of the lariat loop implies that its conformation is essential in stabilizing the basal state of arrestin. The lariat loop is likely to undergo significant structural changes upon activation when the constraints imposed on D290 and D297 are released as the polar core is perturbed. The sequence corresponding to the lariat loop 280–310 in β-arrestin was found to be the major epitope for autoimmune antibodies found at high levels in the sera of some multiple sclerosis patients [19]. The equivalent region in v-arrestin is one of the highly pathogenic epitopes for the autoimmune disease uveoretinitis [20].

The proline-rich regions 88–96 and 120–124 in β-arrestins are responsible for binding to the SH3 domain of c-Src [7]. SH3 domains mediate binding between proteins through hydrophobic interactions via a polyproline helix II (PPII) conformation characterized by ϕ and φ angles of -78° and 149°, respectively [21]. Residues 88–89 do not display a PPII-type conformation. Residues 119–120 and 123–126 display strong characteristics of a canonical PPII, while the intervening P121 and N122 are not in a PPII conformation in the β-arrestin structures. Conceivably, upon arrestin's transition into the active state and receptor binding, these two amino acids undergo the necessary conformational changes to transform residues 119–126 into a continuous PPII that is capable of c-Src binding. This may explain why Src activation by β-arrestin depends on receptor binding. In contrast, the equivalent region in v-arrestin (122–128) does not display any PPII features.

The structural and sequence similarities among all arrestins suggest that receptor binding mechanisms are similar, although details of particular interactions may differ. Thus, mutagenesis results obtained with v-arrestin can be

Table 2. Data Refinement Statistics

Molecule	β-arrestin 1–393	β-arrestin 1–393	β-arrestin 1–382
Space group	$P2_1$	$P3_221$	$P2_1$
Number of reflections (work/free)	65,249/5,401[a]	47,246/5,218	66,013/2,063
Resolution (Å)	35–1.9	33–2.2	33–2.0
R_{work}/R_{free} (%)[b,c]	23.5 (37.9)/26.9 (40.2)	23.9 (35.5)/26.7 (39.2)	25.4 (38.7)/28.0 (38.3)
Mol/ASU	2	1	2
Rms Deviation from Ideality			
Bond angles (°)	1.7	1.6	1.24
Bond length (Å)	0.011	0.01	0.005
Residues/theoretical	713/786	353/393	651/764
Protein atoms	5,657	2,798	5,154
Water atoms	269	102	283

[a] Against combined reference structure factors from SHARP.
[b] Values for the highest resolution shell are given in parentheses.
[c] No rejections based on I/σ(I) ratio.

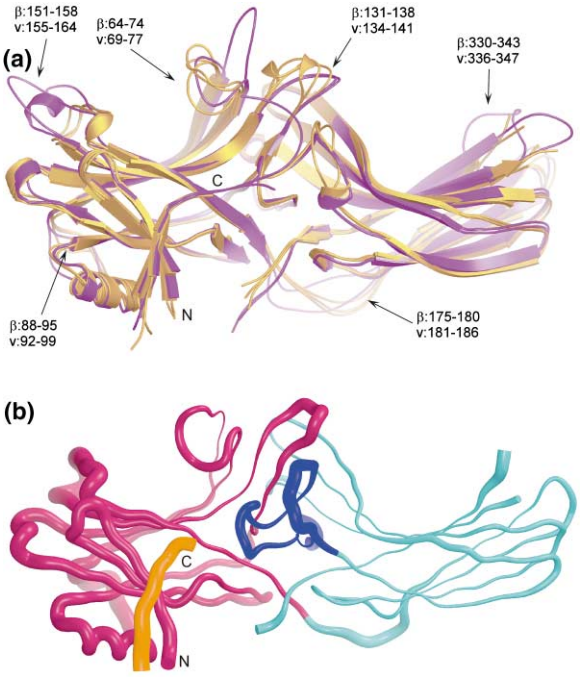

Figure 2. Structural Similarity and B Factor Distribution in Arrestins

(a) Structural alignment between β-arrestin and v-arrestin. A superimposition of β-arrestin 1–393 and v-arrestin structures is shown. The three β-arrestin structures (β) described in this report are shown in gold; v-arrestin (v) α and β [1] are drawn in purple. Highly flexible regions, which vary within and between both families of proteins, are indicated by arrows. Figure generated with MOLSCRIPT/RASTER3D [69, 70].

(b) B factor distribution of β-arrestin. Worm diagram of β-arrestin, $P3_221$ form, along with the B factor encoded in the variable radius. On average, the N domain (purple) displays a higher B factor compared to the C domain (cyan). β-arrestin's C tail (383–392) is depicted in orange, and the lariat region (280–310) is drawn in dark blue. Figure generated in SPOCK/RASTER3D [70].

interpreted in the context of β-arrestin. In addition to their ability to bind to a wide range of GPCRs, β-arrestins are more versatile in downstream effector interactions. They mediate other cellular processes such as activation of the mitogenic pathways through interactions with c-Src [7, 8] and downstream kinases [14] as well as receptor endocytosis through interactions with clathrin and AP2 [3–5].

Analysis of the temperature-factor distribution of arrestins (Figure 2b) shows that the N domain (purple) is considerably more flexible than the C domain (cyan) despite the higher sequence conservation observed in the N domain. This profile is observed throughout all structures of β-arrestin and v-arrestin (data not shown). The other two regions with high-temperature factors are the lariat region (282–309, blue) and the C tail (383–393, orange). The temperature-factor profile strengthens the notion that the N domain, the lariat region, and the C tail undergo substantial conformational rearrangements upon receptor binding, while the more static C domain serves as a structural scaffold. It has been suggested that the polar core is disrupted [1] and the C tail dissociates from arrestin's surface [16, 22–24] upon binding to the receptor.

Dimerization of β-Arrestin

Full-length β-arrestin and the β-arrestin 1–393 truncation mutant both exist as monomers in solution, as assayed by gel-filtration chromatography. In contrast, the only marginally shorter truncation mutant β-arrestin 1–382 exists as a mixture of monomeric and dimeric species (with a ratio of 4 to 1).

The differences in dimerization properties among various constructs of β-arrestin are also reflected in oligomeric states of the molecules in the crystals. Full-length β-arrestin yields only trigonal crystals with one monomer per asymmetric unit, whereas β-arrestin 1–382 yields exclusively monoclinic crystals with one dimer per asymmetric unit. The intermediate β-arrestin 1–393 yields both forms. Most likely, the structure observed in the trigonal crystal form is that of the solution monomer, and the structure in the monoclinic crystal form represents the solution dimer. The two conformations are very similar with the exception of a few loop regions (Figure 2a), and both represent the inactive basal state of the molecule. A dimer of β-arrestin 1–393 in the monoclinic form is shown in Figure 3a. The dimer of β-arrestin 1–382 is essentially identical to that of β-arrestin 1–393.

Monomeric and dimeric forms of v-arrestin are at equilibrium under physiological conditions [25]. It was proposed that the dimer represents an inactive species of v-arrestin, which, upon dissociation, yields active monomer. This would ensure a low steady-state concentration of monomeric arrestin and prevent premature quenching of the signal due to an oversupply of arrestin. Interestingly, the deletion of β-arrestin's C tail enhances dimerization, whereas the equivalent truncation of v-arrestin actually decreases its tendency to dimerize [25]. The dimerization interfaces utilized by the two proteins are different. V-arrestin employs a head-to-tail arrangement, whereby the C domain of one molecule interfaces with the N domain of its binding partner (Figure 3b). In contrast, β-arrestin forms a tail-to-tail dimer, with two C domains interfacing each other (Figure 3a). The buried surface areas [26] for β-arrestin and v-arrestin dimers are 1400 and 2000 $Å^2$, respectively. We believe that the wild-type β-arrestin predominantly exists as a monomer in the cell for two reasons. First, full-length β-arrestin exists as a monomer under physiological conditions; dimerization is only observed for truncated proteins. Second, the intracellular concentration of β-arrestin is likely to be much lower than the concentration of v-arrestin in rod cells (50–170 μM [27, 28]), favoring the monomeric state. Hence, there is a mechanistic difference between v- and β-arrestins regarding activity regulation through self-association. Several lines of evidence indicate that upon receptor binding, arrestin's C tail is displaced [16, 22–24]. It is noteworthy that the removal of the C tail by mutagenesis, mimicking its displacement during receptor binding, promotes β-arrestin dimerization. Displacement of the C tail is most likely also a necessary step before β-arrestin is able to interact with the β2 subunit of the adaptor protein AP-2. Recent studies [29] have shown that the conserved residues R393 and R395 in β-arrestin (R394 and R396 in β-arrestin2) are essential for this interaction. In β-arrestin's basal state, R393 is an integral part of the

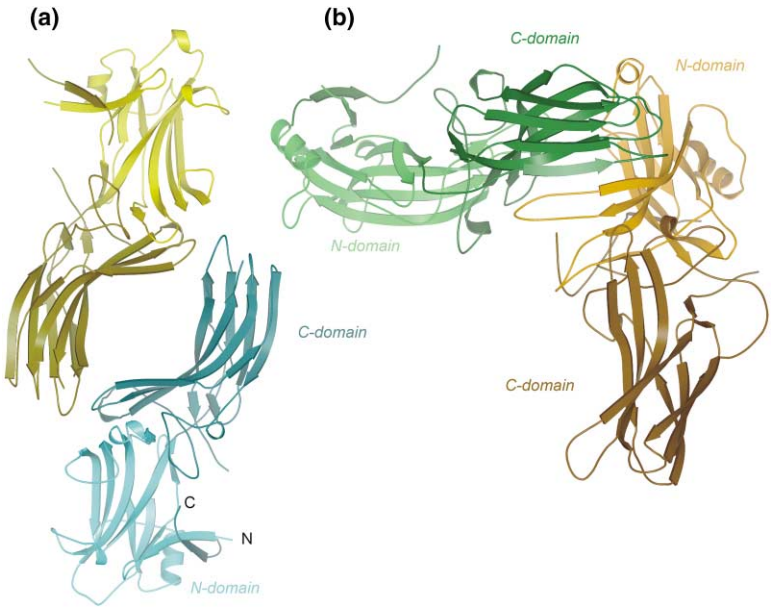

Figure 3. Dimer Interfaces of β-Arrestin and V-Arrestin

(a) Ribbon diagram depicting the dimer interface of β-arrestin 1–393 with the view directly along the two-fold noncrystallographic symmetry axis. α and β forms are drawn in blue and yellow, respectively. The dimer is arranged in a tail-to-tail configuration.

(b) Dimer interface of v-arrestin arranged in a head-to-tail configuration. α is drawn in ochre, β is in green hues.

In both panels the N domain is shown in light colors and the C domain in darker colors of the same hue. The buried surface area is 1400 Å^2 for the β-arrestin dimer and 2000 Å^2 for the v-arrestin dimer.

polar core and therefore unavailable for binding to AP-2. It requires the interaction with the receptor to release both arginines and translocate the β-arrestin-receptor complex to clathrin-coated pits through interaction with AP-2.

Defining the Receptor Binding Site

Visual and β-arrestins display selectivity toward their respective physiological partner receptors. V-arrestin binds to phosphorylated/activated rhodopsin (P-Rh*) with much higher affinity than to phosphorylated/activated m2 muscarinic cholinergic receptor (P-m2 mAchR*). β-arrestin displays the opposite preference (Figure 4a). Segment-swapping experiments demonstrate that substituting residues 50–90 of v-arrestin with the equivalent element of β-arrestin (46–86) is necessary and sufficient to reverse the binding specificity of v-arrestin (Figure 4a). A v-arrestin-based chimera with segment 46–86 from β-arrestin binds P-m2 mAchR* with high affinity, concurrently losing the affinity for P-Rh*. Other nonoverlapping segments covering the entire N domain do not reverse the arrestin-receptor specificity (data not shown). Presumably, the residues responsible for arrestin-receptor specificity are directly involved in receptor binding and are most likely conserved within each subfamily of arrestins but differ between the families. Residues 46–86 are located on the concave side of the N domain (Figure 4c, cyan highlights) corresponding to strands V (residues 52–63) and VI (residues 75–87) (Figure 1). Sequence comparison between visual and β-arrestin shows that the region is highly conserved within each family and displays only a few differences between the two families (Figure 4b). The most pronounced differences are Y47 (L51 in v-arrestin), E50 (G54 in v-arrestin), and R65 (Q69 in v-arrestin), all located on the loops flanking the strictly conserved β strand V (Figure 4c). Another notable difference in this region is between S86 in β-arrestin 1 and V90 in v-arrestin (Figure 4b). Remarkably, a single amino acid mutation V90S eliminates this difference and permits v-arrestin to bind P-m2 mAchR* with similar affinity as β-arrestin without significant concurrent loss of its affinity to P-Rh* (Figure 4a). V90 in v-arrestin interacts with V45, V57, V59, and F118 [1], stabilizing the β strand "sandwich" in the N domain via hydrophobic interactions. In β-arrestin, all the potential partners (V41, V53, V55, and F115) are conserved, but S86 cannot engage in hydrophobic interactions with them. We believe that a relatively rigid N domain, stabilized by V90 and its hydrophobic interacting partners, ensures the best fit in the specialized visual arrestins, whereas a substantially more flexible N domain helps nonvisual arrestins to accommodate their diverse receptor partners. The reverse mutation, S86V in β-arrestin, does not have significant impact on its binding to either P-Rh* or P-m2 mAChR* (Figure 4a).

The basal states of both arrestins are very similar. Their stabilizing elements (the polar core and the 3 element interaction of α helix I, β strand I [residues 6–12], and β strand XX [residues 386–390]) are highly conserved, and analogous mutations in β- and v-arrestins result in similar phenotypes [13, 16]. Despite some differences in detailed receptor-arrestin interactions, this suggests that the arrestins' activation mechanisms are similar, and that structure-function data obtained from one arrestin class are relevant for the other. Recently, Hofmann and coworkers conducted extensive competition assays with overlapping peptides covering the entire v-arrestin sequence [30]. Although none of the peptides bound directly to the receptor, a few effectively inhibited arrestin binding to P-Rh* with an IC_{50} of less than 500 μM. The ability of a peptide to inhibit arrestin-receptor interaction is a strong indication of the corresponding segment's direct involvement in receptor binding. However, other segments involved in receptor binding may not be revealed in competition binding assays using isolated peptides. These peptides may

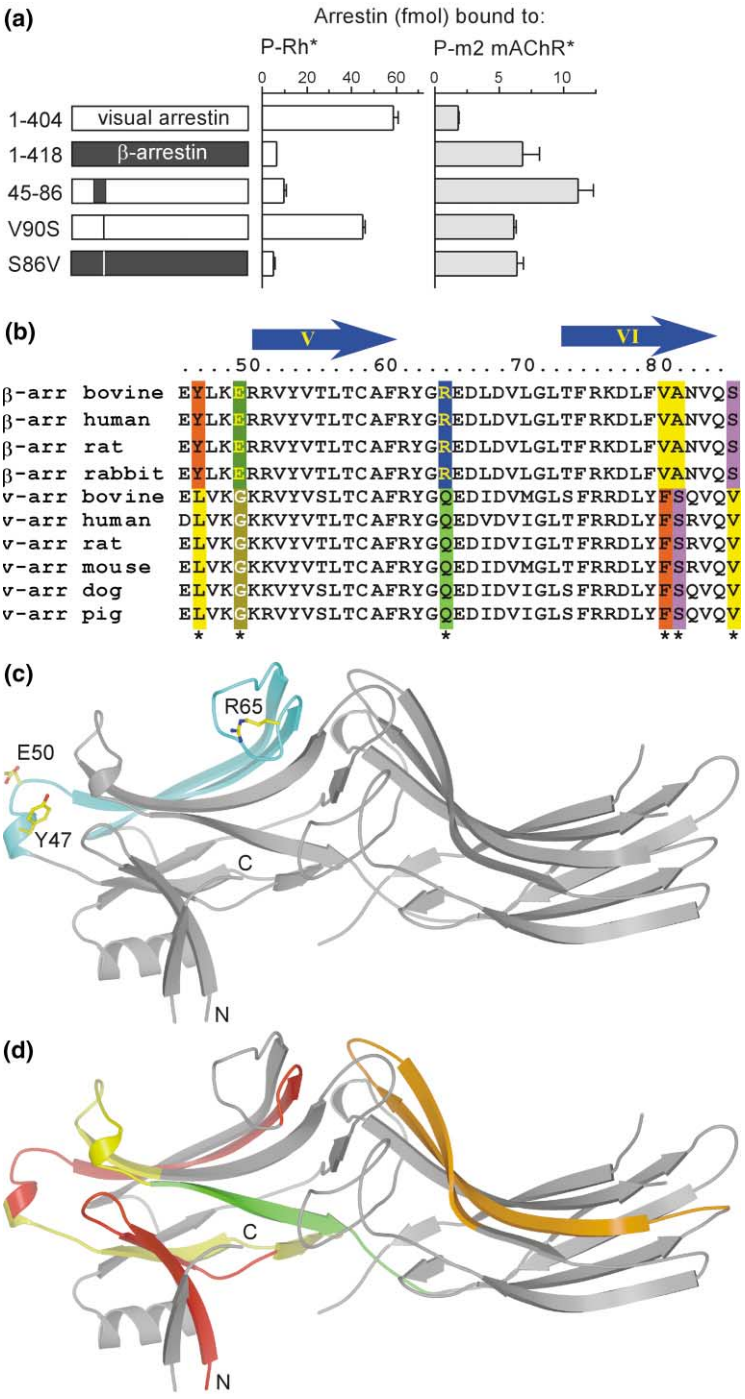

Figure 4. Putative Receptor Binding Sites and Sites Responsible for Receptor Specificity

(a) Segment 46–86 of β-arrestin is necessary and sufficient to reverse the receptor binding specificity of v-arrestin.

(b) Sequence alignment of the 46–84 segment between β-arrestin and v-arrestin families. Two blue arrows signify β strands V and VI. Residues that are conserved within each family but differ between the two are marked with an asterisk.

(c) Residues 45–86 of β-arrestin (highlighted in cyan), when swapped into v-arrestin, dramatically alter v-arrestin's receptor specificity. Side chains of residues conserved within each class of arrestin but differ between the two are shown.

(d) V-arrestin peptides that compete with v-arrestin for rhodopsin are mapped onto the β-arrestin structure. Colors encode the potency of the competition: yellow, $IC_{50} \leq 100$ μM; orange, $100 \leq IC_{50} \leq 200$ μM; and red, $200 \leq IC_{50} \leq 400$ μM. Segment 164–176, highlighted in green, was shown to be inaccessible to antibody interaction upon receptor binding.

be unable to adopt the tertiary structure required for receptor binding in the absence of the buttressing effects of the rest of the protein. We mapped the peptides displaying inhibitory effects onto the structure of β-arrestin (Figure 4d). The most potent peptide 51–70 (44–66 in β-arrestin, yellow) corresponding to β strand V and flanking loops competes with an IC_{50} of 25 μM. It is also a part of the 46–86 region responsible for receptor binding specificity identified by the segment swapping experiments (Figure 4a). Another segment, corresponding to β strand X (residues 170–182 in v-arrestin, 164–172 in β-arrestin; Figure 4d, green), has also been implicated in receptor binding since it becomes inaccessible to antibody interaction upon receptor binding [31]. According to mutagenesis studies, several residues in the same region are directly involved in receptor binding [32, 33]. Interestingly, peptides implicated in receptor binding do not form a contiguous surface (Figure 4d), suggesting that the receptor/arrestin complex may have two or more discrete interfaces. This notion is supported by the finding that multiple receptor elements, cytoplasmic loops 1, 2, and 3 and the C terminus, participate

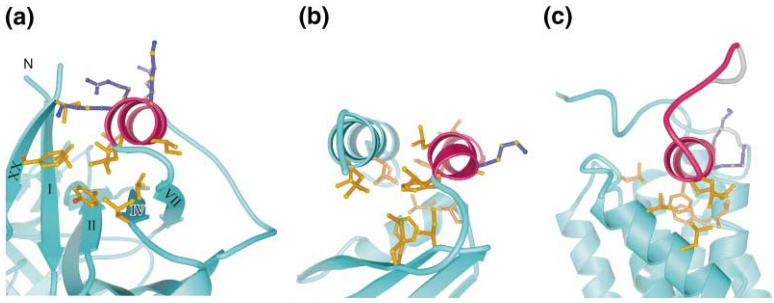

Figure 5. Amphipathic Helices and Their Hydrophobic Interfaces

The amphipathic helices of (a) β-arrestin, (b) ARF1-GDP, and (c) rhodopsin, respectively. The helices (purple) are anchored to the majority of the protein by interactions of hydrophobic residues shown in gold. Hydrophilic residues shown in blue point into the solvent. Disordered parts of the C-terminal segment of rhodopsin (c) are shown in gray.

in arrestin binding [34, 35] and that noncontiguous receptor residues are involved [36].

Possible Roles of the Amphipathic α Helix I in Arrestin Membrane Translocation

All crystal structures of arrestins solved so far represent the basal (inactive) state. Understanding the activation mechanism requires the determination of the structure of an arrestin-receptor complex, which remains to be crystallized. However, structural analysis combined with the interpretation of mutagenesis studies allows us to propose a new element of arrestin's activation mechanism.

Residues 98–108 (α helix I) form a cationic amphipathic helix, where the hydrophobic residues L100, L104, and L108 are perfectly aligned on the same face of the helix. This face is flanked on both sides by four positive charges, R99, R103, K106, and K107 (Figure 5a). The net charge of the helix is +3. Such helices often serve as reversible membrane anchors [37], with the helix axis lying parallel to the bilayer surface, the hydrophobic residues inserting into the membrane, and the positive charges interacting with negatively charged lipid head groups. In the basal state of β-arrestin, as revealed by the crystal structure, the hydrophobic face of α helix I is completely buried in a hydrophobic environment composed of residue V8, the aliphatic chains of K10, Y21, V40, V42, I386, and F388 (Figure 5a). Interactions with β strands I and XX further stabilize this position of α helix I. Receptor binding apparently destabilizes this three element interaction, releasing arrestin's C tail [22, 38] and shifting β strand I out of its resting position [23]. Destabilization of these interactions by alanine substitutions of hydrophobic residues in either C tail (mutant 3A) or β strand I (mutant N3A) dramatically enhances arrestin binding to all forms of rhodopsin: P-Rh*, unphosphorylated light-activated (Rh*), and dark-phosphorylated rhodopsin (P-Rh). In contrast, alanine substitution of leucines in α helix I (mutant h3A) only moderately enhances the binding to P-Rh and Rh*. In the context of 3A and N3A mutants, where the 3 element interaction is already destabilized, mutant h3A demonstrated lower binding to all functional forms of rhodopsin. This suggests that hydrophobic residues in α helix I play an additional binding-enhancing role in the active state of arrestin [23]. We hypothesize that after receptor-induced displacement of its partners, the helix flips out and inserts itself into the membrane, where it serves as an additional membrane anchor and thereby enhances receptor binding. Extended hinges on both sides of α helix I (Figure 5a) provide the flexibility necessary for this structural rearrangement.

Similar activation-induced membrane translocation via a cationic amphipathic helix has been described for ADP-ribosylation factor-1 (ARF1). In the basal state of ARF1-GDP, an amphipathic N-terminal α helix is bound in a hydrophobic core similar to α helix I in β-arrestin (Figure 5b) [39]. The conformational changes associated with activation involve substantial structural rearrangements, as revealed by the structure of the active ARF1-GTP form [40]. As a result of GTP binding, switch 1 transforms from a β hairpin structure to a loop with one residue moving as much as 16 Å. Strands β2 and β3 slide 7 Å toward the N terminus relative to the invariant part of the molecule and occupy the space that hosts the α helix in the basal state. The N-terminal α helix has to move away from its original position to accommodate the new active conformation. Biochemical studies using fluorescence energy transfer showed directly that the displaced amphipathic helix translocates and anchors ARF1 to the cell membrane [41].

Interestingly, H8 of rhodopsin displays the same cationic amphipathic nature. It was shown to lie on the surface of the bilayer with the helical axis parallel to the membrane plane, hydrophobic residues (F313, M317, and L321) penetrating into the hydrophobic portion of the bilayer, and the positive charges (K311 and R315) at the aqueous-membrane boundary ([42]; Figure 5c). The cationic amphipathic character of the segment is well conserved in most of the rhodopsin-family GPCRs (http://www.gpcr.org/7tm/); therefore, the arrangement of H8 is likely to be a common feature of the molecular architecture of GPCRs in addition to the seven transmembrane helices. Moreover, the hydrophobic residues interact not only with lipids, but also with hydrophobic side chains from transmembrane helices (TMH) 1 and 7. The phenyl ring of the highly conserved F313 stacks perfectly with the side chain of Y306, a part of a conserved motif NPxxY in TMH7, implying the functional importance of this interaction. We envision that upon activation, α helix I of arrestin interacts with the membrane in a similar manner as H8 of rhodopsin. The hydrophobic residues thus inserted into the membrane may also interact with TMH side chains of the receptor close to the cytoplasmic-membrane boundary.

Reversible membrane anchorage is a common mechanism for cellular redistribution of proteins in response to activation. Often it enhances the affinity of a soluble protein for its membrane bound partner [37]. Membrane anchors are found in many proteins involved in the GPCR-mediated signal transduction pathway where the

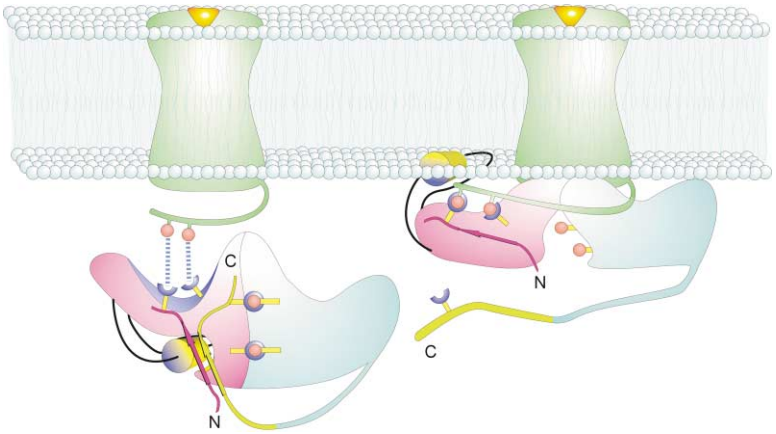

Figure 6. Proposed Receptor Binding Mechanism of β-Arrestin

The cartoon illustrates the proposed receptor binding mechanism of arrestins. The N and C domain are shown in pink and cyan, respectively. The polar core is located at the interface between the N and C domains and is represented by charge-charge interactions (blue-red dots). The C tail is drawn in yellow-green hues, the N-terminal strand I is in magenta. Positive and negative charges are represented by blue and red colors; hydrophobic portions are in yellow. The activated receptor is depicted in green.

primary event happens at the cell membrane. Proteins interacting with GPCRs directly, such as G proteins and receptor kinases, have additional membrane anchors and do not rely solely on receptor binding for their normal function. The individual G protein subunits are subject to prenylation and acylation [43]. Kinases are prenylated and/or bind to the membrane through Gβγ interaction via their PH domains [44]. Regulators of G proteins (RGS) and kinases are translocated to the membrane upon activation via an amphipathic helix [45, 46], very similar to the scenario proposed for arrestins. In the case of recoverin, a Ca^{2+}-myristoyl switch [47] is responsible for membrane binding. Based on structural and functional evidence, we believe that arrestin, binding directly to receptors and organizing many downstream signaling events at the cell membrane, is not an exception and that α helix I serves as its reversible membrane anchor.

Receptor Binding Mechanism

During receptor binding, arrestin undergoes a major conformational rearrangement as judged by the unusually high activation barrier of 140 kJ/mol [48, 49]. We found that the constitutively active mutant β-arrestin 1–382 [16] does not adopt the active conformation in the absence of the receptor. Apparently, arrestin assumes its active conformation only in complex with the receptor. Based on the structures of β-arrestin (this study) and v-arrestin [1] in conjunction with ample biochemical evidence, we propose the following receptor binding mechanism, schematically illustrated in Figure 6.

The inactive conformation is stabilized by an intact polar core and a three element hydrophobic interaction involving β strand I of the N terminus, the last β strand XX of the C terminus, and α helix I (Figure 5a). Upon activation-dependent phosphorylation of GPCRs, an increase in negative electrostatic potential of the receptor attracts cytosolic arrestin through a patch of strong positive potential (shaded blue in Figure 6), which translocates to the membrane and binds to the GPCR. Multiple phosphorylation at the C terminus of the receptor (red dots, Figure 6) is necessary for efficient arrestin binding both in vitro and in vivo [50, 51]. K15 in v-arrestin's β strand I (equivalent to K12 in β-arrestin) directly interacts with receptor-attached phosphates and "guides" them toward the polar core [23]. Here the phosphates disrupt the delicate charge balance between partly buried charged residues and trigger the release of the restraints, which keep β-arrestin in the basal state and initiates further conformational changes most likely similar to those proposed for v-arrestin [1]. Phosphate-induced movement of K15 likely forces the β strand I out of the position in which it is held by hydrophobic interactions with β strand XX and α helix I. Having lost their interacting partner, β strand XX and the C tail dissociate away from their current positions and dislodge R393 from the polar core [23]. This movement of the C tail away from the rest of arrestin increases the accessibility of both the clathrin binding site and AP2 binding site [29, 52]. As the result of the dissociation of β strand XX and the movement of β strand I, α helix I loses stabilizing hydrophobic interactions provided by both partners. We hypothesize that the amphipathic α helix I then swings out from its resting position and interacts with the membrane bilayer to stabilize the receptor-arrestin complex.

Biological Implications

Comparison of the crystal structure of visual arrestin [1, 2] and the high-resolution structure of β-arrestin described here shows that the overall fold of these molecules is very similar. Moreover, all the key intramolecular interactions that hold arrestins in the basal (inactive) state are remarkably conserved. These include the polar core with its main phosphate sensor (Arg169 in β-arrestin), another positive charge (Arg393), and all three negative charges (Asp290, which serves as the primary counterion for Arg169, as well as Asp26 and Asp297). The three element interaction among β strand I, β strand XX of the C tail, and α helix I is virtually identical to the interaction of the homologous elements in visual arrestin. This conservation implies that the mechanism of activation by phosphorylated agonist-activated receptor is very similar in these two arrestins. In view of the conservation of virtually all the residues involved in these interactions in other cloned arrestin proteins [1], we can further infer that these mechanisms are conserved throughout the whole arrestin family. This hypothesis is supported by available mutagenesis data [13, 16] as well as by direct participation of the same parts of visual arrestin and β-arrestin in the interaction with their cognate receptors

([30]; Figure 4). Another notable similarity is the amphipathic nature of α helix I, which we propose is released when the three element interaction is destabilized in the course of receptor binding [23], as well as the flexible hinges which connect this helix to the body of the N domain (Figure 1). This prompted us to hypothesize that α helix I serves as a reversible membrane anchor, further stabilizing the arrestin-receptor complex. Structural similarity of the basal state of v- and β-arrestin, similar functional consequences of many homologous mutations [13, 16, 33, 53], along with the conservation of key residues in other arrestins tempt us to speculate that the structure of the active receptor-bound state (schematically depicted in Figure 6) of all arrestin proteins is also very similar.

Whereas all arrestin proteins bind to activated phosphoreceptors, two nonvisual arrestins perform several other functions that visual arrestin apparently does not have. These functions fall into two groups. First, both nonvisual arrestins directly interact with various components of the trafficking machinery: clathrin [3, 52], clathrin adaptor AP2 [29], and N-ethylmaleimide-sensitive fusion protein (NSF) [6]. Second, nonvisual arrestins serve as scaffolds that participate in the activation of several mitogen-activated protein kinase (MAPK) cascades [14, 54–57]. In particular, both nonvisual arrestins stimulate the signaling from cRaf-1 via MEK1 to ERK1/2 [14, 54, 55]. It appears that arrestins directly interact with cRaf-1 and Erk2, thus facilitating the formation of the cRaf-1, MEK1, Erk2 complex. Similarly, β-arrestin2 serves as a scaffold for the complex of ASK1, MKK4, and JNK3, in which it directly interacts with ASK1 and JNK3 [56, 57]. At physiological expression levels of all the proteins involved, only receptor bound arrestins interact with all these nonreceptor partners, thereby targeting receptors for internalization and linking various GPCRs to MAPK signaling cascades [14, 54–57]. Receptor binding induces a major conformational change in arrestins [23, 48, 50], which includes the displacement of the C tail [22, 23]. Interestingly, in sharp contrast to visual arrestin [1, 25], the deletion of the β-arrestin C tail promotes its dimerization (Figure 3). In all arrestins, deletion of the C tail beyond its interactions with strand I yields "preactivated" constitutively active mutants [13, 16, 22, 50, 53], apparently because it mimics C tail displacement upon receptor binding. Taken together, these data tempt us to speculate that the propensity of active, receptor bound, nonvisual arrestins to dimerize may play a role in assembling arrestin-receptor complexes into dimers and/or higher oligomeres prior to internalization. Moreover, clathrin, AP2, and NSF, with which nonvisual arrestins interact in the process, are assembled into multimeric matrices, so that arrestin dimerization may help arrestin-receptor complexes fit better with the internalization machinery of the coated pit. It is not clear whether dimerization of nonvisual arrestins plays any role in their function as scaffolds for MAPK, but the size of the complexes containing arrestin and MAPK leaves this possibility open as well [54, 55].

Experimental Procedures

Expression and Purification of β-Arrestin and Its Truncation Mutants

cDNAs encoding bovine β-arrestin wild-type, β-arrestin 1–393, and β-arrestin 1–382 truncation mutants were cloned in frame in pTrcHisB vector (Invitrogen) between NcoI and HindIII sites, eliminating the His tag in the original vector. β-arrestins were expressed in *E. coli* strain BL21 codon plus (Invitrogen) in a 15 liter fermentor (Applicon) in 10 liter ECPM1 media [58] at 30°C, pH 7.0, and 25% O_2 saturation. Cells were induced at 10 O.D. (600 nm) with 100 μM IPTG and harvested by centrifugation after 5 hr. Cell pellets were flash frozen in liquid N_2 and stored at −80°C.

The purification was performed at 0°C–4°C. Cells (100 g) were resuspended in 300 ml lysis buffer (50 mM NaCl, 20 mM Tris-HCl [pH 8.5], 10% glycerol, 1 mM phenylmethylsulfofluoride [PMSF], 1 mM benzamidine-HCl, 10 mM ethylenediaminetetraacetic acid [EDTA], 10 mM ethylene glyco-bis (β-aminoethyl ether) N,N,N′,N′-tetraacetic acid [EGTA], 10 mM dithiotreitol [DTT], and seven pellets of Complete™ protease inhibitor cocktail tablets [Boehringer Mannheim]) and lysed by passing through a Microfluidizer (Microfluidics Corp., Newton, MA) 3–4 times at 600 psi. The lysate was cleared by centrifugation at 100,000 × g, and the supernatant was combined with 40 ml Heparin Sepharose (Pharmacia) resin equilibrated with CB50 (50 mM NaCl, 20 mM Tris-HCl (pH 8.5), 10% glycerol, 0.5 mM PMSF, and 2 mM DTT), allowing batch binding for 2 hr under gentle rotation.

The resin was washed extensively with CB100 (100 mM NaCl, 20 mM Tris-HCl [pH 8.5], 10% glycerol, 0.5 mM PMSF, and 2 mM DTT). Wild-type β-arrestin and β-arrestin 1–393 were eluted with 450 μM inositolhexakisphosphate (InP_6) (Sigma) in CB100. β-arrestin 1–382 was eluted with 3 mM InP_6. Fractions containing β-arrestin were pooled, diluted with CB100, and loaded onto three concatenated 5 ml Hi-Trap Heparin Sepharose (Pharmacia) columns. The columns were washed with CB100 and eluted with a linear gradient from 400 mM to 1 M NaCl for 10 column volumes. The fractions containing pure β-arrestin were pooled and concentrated to ~10 mg/ml in 8 ml collodion membranes (MWCO 25 K, Schleicher and Schuell) with frequent mixing and further purified by gel filtration on a Hi-Load 16/60 Superdex 75 column (Pharmacia). The final product was concentrated again to 10 mg/ml for crystallization.

Selenomethionine (SeMet)-labeled β-arrestin was produced in methionine auxotrophic B834 in 12 liter defined MOPS-based medium [59] supplied with 50 mg/L L-SeMet (Sigma). The cells were grown at 30°C and induced at $O.D._{600}$ of 0.6 with 50 μM IPTG and harvested 5 hr later. Purification was carried out using the same procedure described above.

Direct Binding Assay

In vitro transcription, translation, receptor purification, and phosphorylation were performed, as described [13]. Translation of all proteins used for direct binding assay yielded a single radiolabeled band with expected electrophoretic mobility. The stoichiometries of phosphorylation of rhodopsin and m2 muscarinic cholinergic receptor (m2 mAChR) used were 2.8 and 3.3 mol phosphate per mol, respectively. Binding was performed, as described [13]. Briefly, in vitro translated radiolabeled arrestins (50 fmol) were incubated in 50 mM Tris-HCl (pH 7.5), 0.5 mM $MgCl_2$, 1.5 mM dithiothreitol, and 50 mM potassium acetate with 7.5 pmol of phosphorylated light-activated rhodopsin (P-Rh*) or with 100 fmol/assay of carbachol-activated phosphorylated P-m2 mAChR in a final volume of 50 μl for 5 min at 37°C in room light (rhodopsin) or for 35 min at 30°C (P-m2 mAChR). The samples were then cooled on ice and loaded onto 2 ml sepharose 2B columns equilibrated with 10 mM Tris-HCl (pH 7.4), 100 mM NaCl. Bound arrestin eluted with receptor-containing membranes in the void volume (between 0.5 and 1.1 ml). Nonspecific binding (determined in the presence of 0.3 μg liposomes; it did not exceed 0.4 fmol/assay) was subtracted. Means ± standard deviation from three experiments performed in duplicate are presented.

Crystallization

All three crystal forms were prepared by microbatch crystallization at 19°C under oil; occasionally, microseeding was used to improve crystal quality. Usually, 3.5 μl of protein at a concentration of 5 or 7.5 mg/ml in 0.1 M NaCl, 20 mM Tris-HCl (pH 8.5), 1 mM EDTA, 10 mM DTT, and 5% glycerol was mixed 1:1 with the crystallization solution. Crystals in the trigonal space group were grown from 18%–20% PEG 1500, 0.8 M $MgCl_2$, and 0.1 M Tris-HCl (pH 7.5). Crystals were exposed to increasing concentrations of glycerol and were

frozen in liquid propane in 30% glycerol, 12% PEG 1500, 0.4 M $MgCl_2$, 0.1 M NaCl, 50 mM Tris-HCl (pH 7.5), and 10 mM DTT.

Crystals in the monoclinic space group were grown from 12%–14.5% PEG 4000, 0.4 M $BaCl_2$, and 0.1 M Tris-HCl (pH 7.5) and frozen in liquid propane in 36% glycerol, 8% PEG 4000, 0.2 M $BaCl_2$, 0.1 M NaCl, 0.05 M Tris-HCl, and 10 mM DTT.

Data Collection and Phasing

Data were collected at the beamline X25 at NSLS using a Brandeis B4 detector. SAD experiments using selenomethionine-substituted protein were conducted using inverse beam geometry on the peak wavelength of selenium. After processing with DENZO/SCALEPACK [60] intensities were converted to amplitudes using TRUNCATE [61]; FHSCALE [61] was used to scale native to derivative data. The monoclinic crystal form was initially solved by molecular replacement using the fast-direct method as implemented in CNS [62] and one molecule of bovine v-arrestin [1] (residues 10–382) as a search model. This crystal form contains two molecules in the asymmetric unit with the NCS axis positioned almost parallel to the crystallographic *b* axis. Following rigid body refinement, model bias was reduced by solvent flattening in CNS, which was applied to structure factors obtained from a polyalanine model. Selenomethionine sites were identified according to this map and phases from a SIRAS type refinement calculated in SHARP [63]. Solvent flattening and phase extension were performed in SOLOMON [64]. The trigonal crystal form was also initially solved by molecular replacement, which placed one molecule of a rebuilt model of β-arrestin 1–393 in the asymmetric unit. Phases from a SAD-type refinement were calculated in SHARP/SOLOMON. The monoclinic crystal form of β-arrestin 1–382 was solved by molecular replacement.

Model Building and Refinement

The model for all crystal forms was built in O [65]; subsequent refinement steps were performed in CNS by using simulated annealing and restrained individual B factor refinement against the maximum likelihood targets and, where available, external phases. Anisotropic overall B factor refinement, bulk solvent correction, and crossvalidation were used throughout the procedure. Water molecules, obeying hydrogen bonding criteria, were placed via an automated procedure as implemented in CNS and manual positioning. In an attempt to retrieve the missing parts of the model, which represent roughly 8% of the structure, we employed the program BUSTER [66]. The final model for the $P3_221$ form (residues 7–330, 337–356, and 385–393) has a crystallographic R factor of 23.9% and a free R factor [67] of 26.7%; the $P2_1$ form (residues A: 5–332, 341–357, and 383–393; residues B: 5–331, 339–357, and 383–393) has a crystallographic R factor of 23.5% and a free R factor of 26.9%. Noncrystallographic symmetry restraints were used in the initial stages of the refinement. Analysis of model geometry in PROCHECK [68] shows 87.1% of all residues except glycines and prolines in most-favored regions, 11% in additionally allowed regions, and 1.5% in disallowed regions for the monoclinic crystal form. The trigonal crystal form shows 89.9% of residues in the most favored region, 9.2% in additionally allowed regions, and 1% in forbidden regions of the Ramachandran plot.

Acknowledgments

We dedicate this work to the memory of P.B.S. C.S. would like to thank Dr. A. Brünger for support in a critical situation. We thank Dr. F.M. Richards for support and the staff (Dr. L. Berman) at NSLS-X25 for beam time; Dr. J.L. Benovic for purified GRK2; Dr. M.M. Hosey for purified m2 mAChR; Dr. C. Vonrhein for advice on the use of SHARP; Dr. P. Nissen and Dr. Y. Korkhin for discussions; and Dr. T.P. Sakmar for critical reading of the manuscript. Dr. W. Somers, Genetics Institute, kindly provided us with the opportunity to use the BUSTER software. M.H. is a Joan Payson Scholar of the Helen Hay Whitney Foundation. The work at Yale was supported in part by a National Institutes of Health grant GM22324 (to P.B.S.), and the work at Sun Health was supported by National Institutes of Health grants EY011500 and GM63097 (to V.V.G.).

Received: August 9, 2001
Accepted: August 9, 2001

References

1. Hirsch, J.A., Schubert, C., Gurevich, V.V., and Sigler, P.B. (1999). The 2.8 Å crystal structure of visual arrestin: a model for arrestin's regulation. Cell *97*, 257–269.
2. Granzin, J., Wilden, U., Choe, H.W., Labahn, J., Krafft, B., and Buldt, G. (1998). X-ray crystal structure of arrestin from bovine rod outer segments. Nature *391*, 918–921.
3. Goodman, O.B., et al., and Benovic, J.L. (1996). Beta-arrestin acts as a clathrin adaptor in endocytosis of the beta2-adrenergic receptor. Nature *383*, 447–450.
4. Zhang, J., Ferguson, S.S.G., Barak, L.S., Menard, L., and Caron, M.G. (1996). Dynamin and beta-arrestin reveal distinct mechanisms for G protein-coupled receptor internalization. J. Biol. Chem. *271*, 18302–18305.
5. Lin, F.T., et al., and Lefkowitz, R.J. (1997). Clathrin-mediated endocytosis of the beta-adrenergic receptor is regulated by phosphorylation/dephosphorylation of beta-arrestin1. J. Biol. Chem. *272*, 31051–31057.
6. McDonald, P.H., Cote, N.L., Lin, F.T., Premont, R.T., Pitcher, J.A., and Lefkowitz, R.J. (1999). Identification of NSF as a beta-arrestin1-binding protein. implications for beta2-adrenergic receptor regulation. J. Biol. Chem. *274*, 10677–10680.
7. Luttrell, L.M., et al., and Lefkowitz, R.J. (1999). Beta-arrestin-dependent formation of beta2 adrenergic receptor-Src protein kinase complexes. Science *283*, 655–661.
8. Miller, W.E., Maudsley, S., Ahn, S., Khan, K.D., Luttrell, L.M., and Lefkowitz, R.J. (2000). beta-arrestin1 interacts with the catalytic domain of the tyrosine kinase c-SRC. Role of beta-arrestin1-dependent targeting of c-SRC in receptor endocytosis. J. Biol. Chem. *275*, 11312–11319.
9. Lin, F.T., Daaka, Y., and Lefkowitz, R.J. (1998). beta-arrestins regulate mitogenic signaling and clathrin-mediated endocytosis of the insulin-like growth factor I receptor. J. Biol. Chem. *273*, 31640–31643.
10. Conner, D.A., et al., and Seidman, J.G. (1997). beta-Arrestin1 knockout mice appear normal but demonstrate altered cardiac responses to beta-adrenergic stimulation. Circ. Res. *81*, 1021–1026.
11. Bohn, L.M., Lefkowitz, R.J., Gainetdinov, R.R., Peppel, K., Caron, M.G., and Lin, F.T. (1999). Enhanced morphine analgesia in mice lacking beta-arrestin 2. Science *286*, 2495–2498.
12. Sterne-Marr, R., et al., and Benovic, J.L. (1993). Polypeptide variants of beta-arrestin and arrestin3. J. Biol. Chem. *268*, 15640–15648.
13. Gurevich, V.V., et al., and Benovic, J.L. (1995). Arrestin interactions with G protein-coupled receptors. direct binding studies of wild type and mutant arrestins with rhodopsin, beta 2-adrenergic, and m2 muscarinic cholinergic receptors. J. Biol. Chem. *270*, 720–731.
14. Luttrell, L.M., et al., and Lefkowitz, R.J. (2001). Activation and targeting of extracellular signal-regulated kinases by beta-arrestin scaffolds. Proc. Natl. Acad. Sci. USA *98*, 2449–2454.
15. Roman, G., He, J., and Davis, R.L. (2000). kurtz, a novel nonvisual arrestin, is an essential neural gene in Drosophila. Genetics *155*, 1281–1295.
16. Kovoor, A., Celver, J., Abdryashitov, R.I., Chavkin, C., and Gurevich, V.V. (1999). Targeted construction of phosphorylation-independent beta-arrestin mutants with constitutive activity in cells. J. Biol. Chem. *274*, 6831–6834.
17. Parruti, G., Ambrosini, G., Sallese, M., and De Blasi, A. (1993). Molecular cloning, functional expression and mRNA analysis of human beta-adrenergic receptor kinase 2. Biochem. Biophys. Res. Commun. *190*, 475–481.
18. Vishnivetskiy, S.A., Paz, C.L., Schubert, C., Hirsch, J.A., Sigler, P.B., and Gurevich, V.V. (1999). How does arrestin respond to the phosphorylated state of rhodopsin? J. Biol. Chem. *274*, 11451–11454.
19. Ohguro, H., Chiba, S., Igarashi, Y., Matsumoto, H., Akino, T., and Palczewski, K. (1993). Beta-arrestin and arrestin are recog-

nized by autoantibodies in sera from multiple sclerosis patients. Proc. Natl. Acad. Sci. USA *90*, 3241–3245.

20. Gregerson, D.S., Fling, S.P., Obritsch, W.F., Merryman, C.F., and Donoso, L.A. (1989). Identification of T cell recognition sites in S-antigen: dissociation of proliferative and pathogenic sites. Cell. Immunol. *123*, 427–440.
21. Wu, X., et al., and Kuriyan, J. (1995). Structural basis for the specific interaction of lysine-containing proline-rich peptides with the N-terminal SH3 domain of c-Crk. Structure *3*, 215–226.
22. Gurevich, V.V., Chen, C.Y., Kim, C.M., and Benovic, J.L. (1994). Visual arrestin binding to rhodopsin. intramolecular interaction between the basic N terminus and acidic C terminus of arrestin may regulate binding selectivity. J. Biol. Chem. *269*, 8721–8727.
23. Vishnivetskiy, S.A., Schubert, C., Climaco, G.C., Gurevich, Y.V., Velez, M.G., and Gurevich, V.V. (2000). An additional phosphate-binding element in arrestin molecule: implications for the mechanism of arrestin activation. J. Biol. Chem. *275*, 41049–41057.
24. Ohguro, H., Palczewski, K., Walsh, K.A., and Johnson, R.S. (1994). Topographic study of arrestin using differential chemical modifications and hydrogen/deuterium exchange. Protein Sci. *3*, 2428–2434.
25. Schubert, C., Hirsch, J.A., Gurevich, V.V., Engelman, D.M., Sigler, P.B., and Fleming, K.G. (1999). Visual arrestin activity may be regulated by self-association. J. Biol. Chem. *274*, 21186–21190.
26. Lee, B., and Richards, F.M. (1971). The interpretation of protein structures: estimation of static accessibility. J. Mol. Biol. *55*, 379–400.
27. Hamm, H.E., and Bownds, M.D. (1986). Protein complement of rod outer segments of frog retina. Biochemistry *25*, 4512–4523.
28. Kawamura, S. (1995). Phototransduction, excitation and adaption. In Neurobiology and Clinical Aspects of the Outer Retina, M.B.A. Djamangoz, S.N. Archer, and S. Vallerga, eds. (London: Chapman and Hall), pp.105–131.
29. Laporte, S.A., Oakley, R.H., Holt, J.A., Barak, L.S., and Caron, M.G. (2000). The interaction of beta-arrestin with the AP-2 adaptor is required for the clustering of beta 2-adrenergic receptor into clathrin-coated pits. J. Biol. Chem. *275*, 23120–23126.
30. Pulvermüller, A., Schroder, K., Fischer, T., and Hofmann, K.P. (2000). Interactions of metarhodopsin II. arrestin peptides compete with arrestin and transducin. J. Biol. Chem. *275*, 37679–37685.
31. Kieselbach, T., Irrgang, K.D., and Ruppel, H. (1994). A segment corresponding to amino acids Val170-Arg182 of bovine arrestin is capable of binding to phosphorylated rhodopsin. Eur. J. Biochem. *226*, 87–97.
32. Gurevich, V.V., and Benovic, J.L. (1995). Visual arrestin binding to rhodopsin. diverse functional roles of positively charged residues within the phosphorylation-recognition region of arrestin. J. Biol. Chem. *270*, 6010–6016.
33. Gurevich, V.V., and Benovic, J.L. (1997). Mechanism of phosphorylation-recognition by visual arrestin and the transition of arrestin into a high affinity binding state. Mol Pharmacol. *51*, 161–169.
34. Krupnick, J.G., Gurevich, V.V., Schepers, T., Hamm, H.E., and Benovic, J.L. (1994). Arrestin-rhodopsin interaction. multi-site binding delineated by peptide inhibition. J. Biol. Chem. *269*, 3226–3232.
35. Raman, D., Osawa, S., and Weiss, E.R. (1999). Binding of arrestin to cytoplasmic loop mutants of bovine rhodopsin. Biochemistry *38*, 5117–5123.
36. Nakamura, K., Liu, X., and Ascoli, M. (2000). Seven non-contiguous intracellular residues of the lutropin/choriogonadotropin receptor dictate the rate of agonist-induced internalization and its sensitivity to non-visual arrestins. J. Biol. Chem. *275*, 241–247.
37. Johnson, J.E., and Cornell, R.B. (1999). Amphitropic proteins: regulation by reversible membrane interactions. Mol. Membr. Biol. *16*, 217–235.
38. Palczewski, K., Pulvermüller, A., Buczylko, J., and Hofmann, K.P. (1991). Phosphorylated rhodopsin and heparin induce similar conformational changes in arrestin. J. Biol. Chem. *266*, 18649–18654.
39. Amor, J.C., Harrison, D.H., Kahn, R.A., and Ringe, D. (1994). Structure of the human ADP-ribosylation factor 1 complexed with GDP. Nature *372*, 704–708.
40. Goldberg, J. (1998). Structural basis for activation of ARF GTPase: mechanisms of guanine nucleotide exchange and GTP-myristoyl switching. Cell *95*, 237–248.
41. Antonny, B., Beraud-Dufour, S., Chardin, P., and Chabre, M. (1997). N-terminal hydrophobic residues of the G-protein ADP-ribosylation factor-1 insert into membrane phospholipids upon GDP to GTP exchange. Biochemistry *36*, 4675–4684.
42. Palczewski, K., et al., and Miyano, M. (2000). Crystal structure of rhodopsin: a G protein-coupled receptor. Science *289*, 739–745.
43. Lambright, D.G., Sondek, J., Bohm, A., Skiba, N.P., Hamm, H.E., and Sigler, P.B. (1995). The 2.0 Å crystal structure of a heterotrimeric G protein. Nature *379*, 311–319.
44. Inglese, J., Koch, W.J., Caron, M.G., and Lefkowitz, R.J. (1992). Isoprenylation in regulation of signal transduction by G-protein-coupled receptor kinases. Nature *359*, 147–150.
45. Chen, C., Seow, K.T., Guo, K., Yaw, L.P., and Lin, S.C. (1999). The membrane association domain of RGS16 contains unique amphipathic features that are conserved in RGS4 and RGS5. J. Biol. Chem. *274*, 19799–19806.
46. Bernstein, L.S., Grillo, A.A., Loranger, S.S., and Linder, M.E. (2000). RGS4 binds to membranes through an amphipathic alpha-helix. J. Biol. Chem. *275*, 18520–18526.
47. Ames, J.B., Ishima, R., Tanaka, T., Gordon, J.I., Stryer, L., and Ikura, M. (1997). Molecular mechanics of calcium-myristoyl switches. Nature *389*, 198–202.
48. Schleicher, A., Kühn, H., and Hofmann, K.P. (1989). Kinetics, binding constant, and activation energy of the 48-kDa protein-rhodopsin complex by extra-metarhodopsin II. Biochemistry *28*, 1770–1775.
49. Pulvermüller, A., Maretzki, D., Rudnicka-Nawrot, M., Smith, W.C., Palczewski, K., and Hofmann, K.P. (1997). Functional differences in the interaction of arrestin and its splice variant, p44, with rhodopsin. Biochemistry *36*, 9253–9260.
50. Gurevich, V.V., and Benovic, J.L. (1993). Visual arrestin interaction with rhodopsin. sequential multisite binding ensures strict selectivity toward light-activated phosphorylated rhodopsin. J. Biol. Chem. *268*, 11628–11638.
51. Mendez, A., et al., and Chen, J. (2000). Rapid and reproducible deactivation of rhodopsin requires multiple phosphorylation sites. Neuron *28*, 153–164.
52. Krupnick, J.G., Goodman, O.B., Jr., Keen, J.H., and Benovic, J.L. (1997). Arrestin/clathrin interaction. Localization of the clathrin binding domain of nonvisual arrestins to the carboxy terminus. J. Biol. Chem. *272*, 15011–15016.
53. Gurevich, V.V., Pals-Rylaarsdam, R., Benovic, J.L., Hosey, M.M., and Onorato, J.J. (1997). Agonist-receptor-arrestin, an alternative ternary complex with high agonist affinity. J. Biol. Chem. *272*, 28849–28852.
54. DeFea, K.A., Vaughn, Z.D., O'Bryan, E.M., Nishijima, D., Dery, O., and Bunnett, N.W. (2000). The proliferative and antiapoptotic effects of substance P are facilitated by formation of a beta-arrestin-dependent scaffolding complex. Proc. Natl. Acad. Sci. USA *97*, 11086–11091.
55. DeFea, K.A., Zalevsky, J., Thoma, M.S., Dery, O., Mullins, R.D., and Bunnett, N.W. (2000). beta-arrestin-dependent endocytosis of proteinase-activated receptor 2 is required for intracellular targeting of activated ERK1/2. J. Cell Biol. *148*, 1267–1281.
56. McDonald, P.H., et al., and Lefkowitz, R.J. (2000). Beta-arrestin 2: a receptor-regulated MAPK scaffold for the activation of JNK3. Science *290*, 1574–1577.
57. Miller, W.E., McDonald, P.H., Cai, S.F., Field, M.E., Davis, R.J., and Lefkowitz, R.J. (2001). Identification of a motif in the carboxyl terminus of beta-arrestin2 responsible for activation of JNK3. J. Biol. Chem. *276*, 27770–27777.
58. Coligan, J.E., Dunn, B.M., Ploegh, H.L., Speicher, D.W., and Wingfield, P.T. (1999) Current Protocols in Protein Science. (New York: John Wiley & Sons).
59. Neidhardt, F.C., Bloch, P.L., and Smith, D.F. (1974). Culture medium for enterobacteria. J. Bacteriol. *119*, 736–747.
60. Otwinowski, Z., and Minor, W. (1997). Processing of X-ray diffraction data collected in oscillation mode. In Methods in Enzy-

mology, Volume 276, C.W. Carter, Jr. and R.M. Sweet, eds. (New York: Academic Press), pp. 307–325.
61. CCP4 (Collaborative Computational Project 4) (1994). The CCP4 suite: programs for protein crystallography. Acta Crystallogr. D *50*, 760–763.
62. Brünger, A.T., et al., and Warren, G.L. (1998). Crystallography and NMR system: a new software suite for macromolecular structure determination. Acta Crystallogr. D *54*, 905–921.
63. de La Fortelle, E., and Bricogne, G. (1997). Maximum-likelihood heavy atom parameter refinement for multiple isomorphous replacement and multiwavelength anomalous diffraction methods. In Methods in Enzymology, Volume 276, C.W. Carter, Jr. and R.M. Sweet, eds. (New York: Academic Press), pp. 472–494.
64. Abrahams, J.P., and Leslie, A.G.W. (1996). Methods used in the structure determination of bovine mitochondrial F-1 ATPase. Acta Crystallogr. D *52*, 30–42.
65. Jones, T.A., Zou, J.-Y., Cowan, S.W., and Kjeldgaard, M. (1991). Improved methods for building protein models in electron density maps and the location of errors in these models. Acta Crystallogr. A *47*, 110–119.
66. Bricogne, G. (1997). Bayesian statistical viewpoint on structure determination: basic concepts and examples. In Methods in Enzymology, Volume 276, C.W. Carter, Jr. and R.M. Sweet, eds. (New York: Academic Press), pp. 361–423.
67. Brünger, A.T. (1992). Free R-value—a novel statistical quantity for assessing the accuracy of crystal-structures. Nature *355*, 472–475.
68. Laskowski, R.A., MacArthur, M.W., Moss, D.S., and Thornton, J.M. (1993). PROCHECK: a program to check the stereochemical quality of protein structures. J. Appl. Crystallogr. *26*, 283–291.
69. Kraulis, P. (1991). MOLSCRIPT: a program to produce both detailed and schematic plots of protein structures. J. Appl. Crystallogr. *24*, 946–950.
70. Merritt, E.A., and Bacon, D.J. (1997). Raster3D: photorealistic molecular graphics. In Methods in Enzymology, Volume 277, C.W. Carter, Jr. and R.M. Sweet, eds. (New York: Academic Press), pp. 505–524.

Accession Numbers

The coordinates and structure factors have been deposited in the Protein Data Bank with the accession codes 1G4M and 1G4R for the $P2_1$ and $P3_221$ crystal forms, respectively.